High-Resolution Spectroscopy of Ursa Major Moving Group Stars[1,2]

Jeremy R. King & Simon C. Schuler

Department of Physics and Astronomy, 118 Kinard Laboratory, Clemson University, Clemson, SC 29634-0978

jking2,sschule@ces.clemson.edu

ABSTRACT

We use new and extant literature spectroscopy to address abundances and membership for UMa moving group stars. We first compare the UMa, Coma, and Hyades H-R diagrams via a homogeneous set of isochrones, and find that these three aggregates are essentially coeval; this (near) coevality can explain the indistinguishable distributions of UMa and Hyades dwarfs in the chromospheric emission versus color plane. Our spectroscopy of cool UMa dwarfs reveals striking abundance anomalies–trends with $T_{\rm eff}$, ionization state, and excitation potential–like those recently seen in young cool M34, Pleaides, and Hyades dwarfs. In particular, the trend of rising λ7774-based O I abundance with declining $T_{\rm eff}$ is markedly subdued in UMa compared to the Pleiades, suggesting a dependence on age or metallicity. Recent photometric metallicity estimates for several UMa dwarfs are markedly low compared to the group's canonical metallicity, and similar deviants are seen among cool Hyads as well. Our spectroscopy does not confirm these curious photometric estimates, which seem to be called into question for cool dwarfs. Despite disparate sources of Li data, our homogeneous analysis indicates that UMa members evince remarkably small scatter in the Li-$T_{\rm eff}$ plane for $T_{\rm eff}\geq$5200 K. Significant star-to-star scatter suggested by previous studies is seen for cooler stars. Comparison with the consistently determined Hyades Li-$T_{\rm eff}$ trend reveals differences qualitatively consistent with this cluster's larger [Fe/H] (and perhaps slightly larger age). However, quantitative comparison with

[1]This paper includes data taken at The McDonald Observatory of The University of Texas at Austin.

[2]Based on observations obtained at Kitt Peak National Observatory, a division of the National Optical Astronomy Observatories, which is operated by the Association of Universities for Research in Astronomy, Inc. under cooperative agreement with the National Science Foundation.

standard stellar models indicates the differences are smaller than expected, suggesting the action of a fourth parameter beyond age, mass, and [Fe/H] controlling Li depletion. The UMa-Coma cool star Li abundances may show a slight 0.2 dex difference; however, this may be mass-independent, and thus more consistent with a modest initial Li abundance difference.

Subject headings: open clusters and associations: general — stars: abundances — stars: evolution — stars: late-type

1. Introduction

The complex patterns exhibited by Li abundances in solar-type stars present an ongoing challenge to our fundamental understanding of stellar physics, spectral line formation, and Galactic chemical evolution. Open clusters are important objects for deciphering these patterns since they provide a large number of stars with presumably identical heavy element composition, initial Li abundance, but differing mass; moreover, these objects can be accurately dated– at least in a relative sense. Open clusters thus provide a unique and valuable means to study two critical problems related to stellar Li abundances: a) the large star-to-star scatter seen in late-G and K dwarfs and connections to scatter in other stellar properties (Soderblom et al. 1993a; King, Krishnamurthi & Pinsonneault 2000), and b) deconvolving the effects of age-dependent main-sequence depletion and opacity-dependent pre-main-sequence depletion mechanisms in producing intercluster differences in the Li-mass profile (Soderblom 1993b, Swenson et al. 1994, Piau & Turck-Chieze 2002).

Soderblom et al. (1993b) have noted the important niche in such attempts played by the UMa moving group: most notable is its ability to serve as a proxy for a cluster with an age presumably intermediate to the nearby and well-studied Pleaides and Hyades clusters, but having a subsolar "metallicity" (-0.08; Boesgaard, Budge, & Burck 1988; Boesgaard & Friel 1990) lower than either cluster. Li abundances in the UMa moving group have been studied previously by Boesgaard, Budge & Burck (1988) and Soderblom et al. (1993b). The intervening decade following these studies has seen the availability of new UMa star data– activity measures, radial velocities, photometry, Hipparcos parallaxes, etc– which can be used to refine moving group membership. Here, we use new membership information, homogeneously-analyzed abundance data from the literature, and original spectroscopy of our own to revisit Li abundances in the UMa group.

2. Data and Analysis

We pulled our UMa stellar sample from the recent membership study of King et al. (2003). Stars with probable and possible final membership status (their 'Y' and 'Y?' classes) were selected, and Li measurements searched for in the literature. Table 7 lists the full sample of stars considered here, their $B-V$ color (from the tabulation in King et al. (2003), projected rotational velocity, Ca II chromospheric emission index, λ6707 Li I equivalent widths, effective temperatures, LTE Li abundances, and associated references. Several of the Li measurements are actually for the Li I and neighboring λ6707.4 Fe I feature. These cases were noted and corrected for in the analysis.

Seven additional UMa candidates from King et al. (2003) were selected for spectroscopic study utilizing new original data. HD 28495, 59747, and 173950 were classified by King et al. (2003) as members. The stars HD 63433 and 75935 were deemed kinematic members, but photometric membership was ambiguous. HD 81659 and 167389 were considered kinematic non-members, but Montes et al. (2001) classified them as kinematic members; our hope was to bring abundance data to bear on the issue of membership for the latter four stars. These 7 additional stars are listed at the bottom of Table 7.

We obtained spectroscopy of 3 of the additional UMa candidates in October 2004 with the "2dcoude" cross-dispersed echelle spectrometer on the 2.7m Harlan J. Smith Telescope at McDonald Observatory and a thinned Tektronix 2048×2048 CCD having 24 μm pixels. Use of the folded Schmidt camera and chosen slit yielded a 2-pixel spectral resolution of $R\sim60,000$. The resulting per pixel S/N values in the continuum regions near the 6707 Å Li I region were 200, 240, and 310 for HD 28495, 167389, and 173950. Spectroscopy of the other 4 additional UMa candidates was secured in December 2004 with the Cassegrain echelle spectrograph on the KPNO 4m. The instrumental setup consisted of the 58-63 echelle grating, 226-1 cross disperser, long-focus camera, and T2KB Tektronix 2048×2048 CCD; a 0.9 arcsec slit width yielded a spectral resolution of $R\sim40,000$. The per pixel S/N values in the Li I region were 465, 235, 270, and 155 for HD 59747, 63433, 75935, and 81659. Data reduction was carried out with standard routines in the IRAF package. Sample spectra are shown in Figure 1. Equivalent widths were measured with the profile fitting routines in the 1-d spectral analysis package SPECTRE (Fitzpatrick & Sneden 1987), and are listed in Tables 1, 3, 5, 6, and 7. Fig. 1 Tab. 1

Li abundances were determined from the equivalent widths using the LIFIND software package kindly provided by Dr. A. Steinhauer (2003). The program determines a color-based effective temperature

$$T_{\rm eff} = 8344 - 3631.32\times(B-V) - 2211.81\times(B-V)^2 + 3265.44\times(B-V)^3 - 1033.62\times(B-V)^4 + 701.7\times(B-V)\times($$

This relation is a slightly higher order fit to the same calibrating data used by Deliyannis, Steinhauer & Jeffries (2002); the zero-point and metallicity terms are discussed by Deliyannis et al. (1994). Interpolating within an internal library of curves of growth generated by the LTE analysis package MOOG using Kurucz (1992; private communication) model atmospheres, LIFIND then returns a Li abundance for a given input equivalent width and $T_{\rm eff}$. When required, LIFIND also corrects the Li abundance for contributions in the λ6707.4 region typically dominated by an Fe I feature; we assumed [m/H]$= -0.08$ for these corrections. For stars with multiple Li measurements, we simply averaged the resulting abundances together. The Li abundance uncertainties listed in Table 7 are internal values comprising contributions due to internal $T_{\rm eff}$ uncertainties from photometric uncertainties and to equivalent width uncertainties. The latter were gauged from multiple measurements, taken from listed uncertainties in the original sources, or calculated from reported S/N, instrumental dispersion, and spectral resolution (or FWHM in the case of non-negligibly rotating stars) values via the formalism of Cayrel (1988). If one wishes to consider the absolute Li abundances alone or compare these to other analyses using different $T_{\rm eff}$ scales, then a larger total $T_{\rm eff}$ uncertainty of $\sim$100 K is more appropriate. This increases the Li abundance uncertainties by $\sim$0.05 dex given the $T_{\rm eff}$ sensitivity of the derived Li abundance in our stars (a change of $\pm$0.12 dex and $\pm$0.09 dex in log N(Li) for a change of $\pm$100 K in $T_{\rm eff}$ at 5100 and 5750 K, respectively).

The derivation of O, Ca, Cr, Fe, and Ni abundances in our 7 additional UMa candidates proceeded as follows. $T_{\rm eff}$ values were taken from above and combined with log g values from Yale-Yonsei isochrones (see next section). Microturbulent velocities were then calculated from the relation of Allende Prieto et al. (2004). These stellar parameters and the overall metallicity of the model atmosphere are listed in Table 2. The lines listed in Tables 1 and 3 are allegedly clean "case a" lines from Thevenin (1990), from which we also took oscillator strengths. We carried out a differential analysis relative to Sun in order to minimize the effects of oscillator strength errors. This was done by measuring the same lines in a spectrum of the zenith daytime sky obtained at the McDonald 2.7m during our October 2004 run, and analyzing them in the same fashion. Abundances were derived using the 2002 version of the LTE analysis package MOOG and Kurucz (1992; private communication) model atmospheres. Absolute solar abundances, log N(X), and relative stellar abundances normalized to solar values on a line-by-line basis, [X/H], are given in Tables 2 and 4. Table 5 contains our O results from the high excitation λ7774 triplet. Table 6 contains our results for Fe II; while the λ6416 Fe II feature appears clean and unblended in all of our spectra (and high resolution solar atlases), the behavior of its associated abundances relative to those from the other 3 lines may suggest mild contamination of the former by another low excitation transition.

The neutral lines of Ca, Cr, Fe, and Ni demonstrate a derived abundance sensitivity

of ±0.05 and ±0.08 dex for a ±100 K change in $T_{\rm eff}$ at 5100 and 5750 K, respectively. The corresponding O sensitivities are ∓0.13 and ∓0.09 dex; those for Fe II are ∓0.10 and ∓0.04 dex. These sensitivities, the internal $T_{\rm eff}$ uncertainties of ∼45 K, and the small internal mean measurement uncertainties (typically a couple hundredths of a dex), yield total internal uncertainties in [X/H] for all species in the 0.05-0.08 range. As for Li, these uncertainties are appropriate for examining star-to-star scatter. For the purpose of external comparisons, total $T_{\rm eff}$ uncertaines of ∼100 K are more appropriate. These bring total abundance uncertainties to the 0.10-0.12 dex level. Tab. 2 Tab. 3 Tab. 4 Tab. 5 Tab. 6

3. Results and Discussion

3.1. The Relative Age of UMa

Before discussing age-related implications of the UMa Li-$T_{\rm eff}$ morphology, it is useful to revisit the relative age of UMa and two key clusters– the Hyades and Coma Berenices. The right hand panel of Figure 2 shows the color-magnitude diagram of the Hyades using the "high fidelity" sample and *Hipparcos* parallaxes from de Bruijne, Hoogerwerf & de Zeeuw (2001). The lines are the 500, 700, and 900 Myr, [Fe/H]= +0.13, [α/Fe]= 0 Yale-Yonsei isochrones (Yi et al. 2001) using the Lejeune et al. (1998) color-$T_{\rm eff}$ relations. The left hand panel shows the photometry from the final *Hipparcos*-based UMa member sample of King et al. (2003) and the [Fe/H]= −0.08, [α/Fe]= 0 Yale-Yonsei isochrones for 400, 600, and 800 Myr (all using the Lejeune et al. 1998 color-temperature relations). Fig. 2

Earlier inhomogeneous age estimates placed the Hyades-UMa age difference at 300-500 Myr. The homogeneous comparison in Figure 2 suggests that this age difference is, in fact, considerably smaller– ≤100 Myr, but the uncertainties may even allow coevality. Assuming a significant UMa-Hyades age difference, Soderblom & Clements (1987) called attention to the seemingly remarkable similarity of the mean UMa and Hyades chromospheric emission levels. Scatter in the UMa emission levels is also significantly smaller than in younger clusters such as the Pleiades (e.g., Figure 11 of King et al. 2003). A similar age for UMa and the Hyades, suggested here, at last provides a natural explanation for these observations.

The left hand panel of Figure 3 shows again the UMa color-magnitude diagram, while the right hand panel shows that for the Coma Berenices cluster. The Coma photometry is from Johnson & Knuckles (1955) and Ford et al. (2001), and the assumed reddening of $E(B-V) = 0$ and distance modulus of 4.54 are taken from Pinsonneault et al. (1998). Given a Coma metal abundance of [Fe/H]= −0.07 (Boesgaard 1989), we utilized the same isochrones displayed in the UMa diagram. The Coma-UMa age comparison in Figure 3

suggests that these two systems too are essentially coeval. Fig. 3

3.2. Metal Abundances and Membership

Table 7 lists photometric and spectroscopic [Fe/H] values for our UMa stars. The former are Stromgren-based values from the recent large survey of Nordstrom et al. (2004). The latter are taken from literature values tabulated in **?** or, for the additional UMa stars at the bottom of the table, our own results in Tables 2 and 4. There are several stars for which the photometric metallicity is notably lower than the canonical spectroscopic value of [Fe/H]= −0.09 (Boesgaard & Friel 1990): HD 11131 (-0.27), 109799 (-0.24), 184960 (-0.32), 28495 (-0.41), and 173950 (-0.43). As a check on these photometric metallicities, we calculated the mean abundance of Hyades members in the Nordstrom et al. (2004) catalog using the cluster membership list of Perryman et al. (1998) culled of questionable members. The result is [Fe/H]= −0.01 with a star-to-star scatter of 0.14 dex; this mean, which is raised by only 0.02 dex if spectroscopic binaries and radial velocity variables are excluded, is some ∼0.15 dex lower than the canonical spectroscopic Hyades metallicity. It is not clear that the Nordstrom et al. (2004) abundance data are robust enough to address UMa membership. Tab. 7

From our own spectroscopic abundance results in Tables 2 and 4, several things seem clear. First, the line-to-line scatter in the abundances is satisfyingly small. This suggests that insidious effects noted by King et al. (2000), such as differential blending in the Sun relative to the cooler additional UMa stars, is not important here. However, an example of the pitfalls awaiting the unwary spectroscopist is provided by the λ6417 Ca I line, which is blended in our cool UMa candidates, but apparently clean in the Sun. The blend is subtle, particularly given finite S/N, but identified from the consistent appearance of the line profile in all cool stars and consistently grossly deviant abundances. It is possible that a few, even more subtle, "clunkers" have escaped detection and reside in Table 1 and 3. We simply note again that differential blending is a potential pitfall in differential analyses of cool stars–particularly when using lines from a Sun-based line list.

Second, both the photometric and our own spectroscopic abundances indicate that HD 81659 is markedly metal-rich compared to true UMa group stars. Given our earlier kinematic non-membership assignment, we eliminate it as an UMa group member. Indeed, its Li abundance is markedly lower than UMa stars of similar $T_{\rm eff}$ (see below).

Third, the markedly low photometric abundances for HD 28495 and 173950 are not confirmed by spectroscopic analysis. Our [Fe/H] values are some ∼0.25 dex higher. While considerably more analysis with larger samples of stars is needed, this could signal a problem

with the photometric determinations of cool ($T_{\rm eff}\leq$5200 K) stars; indeed, the markedly low photometric [Fe/H] values for Hyades members from Nordstrom et al. (2004) seem to occur preferentially at the cool end.

Fourth, striking evidence for overexcitation/ionization is clearly seen in our cool UMa stars. A growing body of work (Schuler et al. 2003, 2004; Morel & Micela 2004; Morel et al. 2004; Yong et al. 2004) building on earlier suggestions (Cayrel et al. 1985, King et al. 2000) indicates that cool dwarf abundances show excitation and ionization-related anomalies when subjected to LTE analysis with standard stellar photospheric models. This behavior is seen in our stars: the Ca abundances derived from the higher excitation λ6417 feature (measured to account for the blending noted above) are consistently higher than derived from other Ca transitions for the cool stars in Table 4; the Cr abundancs derived from the lower excitation λ6330 feature are consistently lower than derived from other Cr transitions in all cases (Table 4). The Fe I abundances derived from the lower excitation λ6498 feature are lower than derived from higher excitation features in all cases (Table 4). More marked is the Fe II−Fe I difference–a stunning 0.42 dex for the four coolest objects in Table 6.

Figure 4 shows the Fe II-Fe I differences (see Table 6) and high excitation (9 eV) λ7774 triplet-based [O/H] values (see Table 5) versus $T_{\rm eff}$ for HD 28495, 59747, 63433, 75935, 167389, and 173950 derived from our new spectroscopy. There is a clear trend with Teff, and that for O I appears notably more shallow than for the Pleiades. These striking trends are qualitatively similar to those for [O/H] and Fe I-Fe II seen by Schuler et al. (2003, 2004) and Yong et al. (2004) for M34, the Pleiades, and the Hyades. Whether the shallower slope of the O I trend for our UMa stars compared to the Pleiades is somehow related to the former's larger age or lower metallicity is unclear, and will require observations of additional clusters/moving groups. Fig. 4

We believe that the anomalous abundance results for cool stars like that shown in Figure 4 are not explained by simple modest parameter variations. For example, the large O I abundances and Fe II-Fe I differences could be removed by lowering log g by in the cool stars– but by a full dex. Raising the overall $T_{\rm eff}$ scale for all the UMa stars by 900-1000 K would also flatten out the observed trends in [O/H] and Fe ionization state difference. An alternative fix is to raise the $T_{\rm eff}$ values of the 4 coolest stars by 250 K with respect to the stars near solar $T_{\rm eff}$. An analogous solution to removing the [O/H] trend in the Pleiades (Schuler et al. 2004), however, would require the cool star $T_{\rm eff}$ values to be increased by several factors of 250 K. We regard all these parameter variations as implausible.

Given the totality of the evidence in Tables 2 and 4, our abundances only rule out membership for HD 81659. A remaining possible curiosity is that the Fe abundances of HD 59747 are consistently slightly higher on a line-by-line basis compared to the similarly cool

dwarfs HD 75935 and HD 173950; this is true for Fe II as well. Such behavior, however, is not clearly seen in (e.g.,) Ca, Cr, or Ni. Additional work is needed to understand how these striking anomalies noted above might also vary from star-to-star at a given $T_{\rm eff}$, a possibility if activity were an underlying cause (as suggested by, e.g. Morel & Micela 2004 and Morel et al. 2004), within an otherwise uniform population. In the meantime, we note that the slightly low mean Fe abundances for the cool stars HD 28495 and HD 173950, the larger Fe abundances for the warmer dwarfs HD 63433 and HD 167389, and low mean Ca values for the cool stars HD 75395, 59747, and 173950 (all compared to the canonical UMa metallicity of [m/H]~ -0.09) that one might notice from Tables 2 and 4 are exactly what one expects given the overexcitation/ionization effects seen in, e.g., M34 (Schuler et al. 2003).

3.3. Li in the UMa Group

The Li-$T_{\rm eff}$ morphology of our UMa members (those stars in Table 7 with the exception of HD 81659) is shown in Figure 5. Barring the three clear members of the Li gap at 6400-6700 K, a notable feature seen here is the lack of statistically significant star-to-star scatter in the Li abundances for Teff$\geq$5200 K; in this regime the spread in Li is remarkably small– especially when considering the inhomogeneous data sources. Scatter about a fitted polynomial (excluding Li gap stars) is only a few hundredths of a dex– that expected from the uncertainties in Table 7. Fig. 5

A second feature of note is that the 0.4-0.5 dex difference between the UMa Li abundances on the hot side of the F-star Li gap and the so-called Li peak at 5800-6000 K is consistent with that in the older Hyades and Coma clusters (e.g., Figure 3 of Jones et al. 1997 and Figures 5 and 6 below) rather than the near-zero difference seen in the Pleiades (e.g., Figure 3 of King, Krishnamurthi, & Pinsonneault 2000). This is consistent with similar ages for UMa, Coma, and the Hyades as we infer from their color-magnitude diagrams.

Below $T_{\rm eff}\sim$5200, Figure 5 indicates that there exists significant star-to-star scatter. Figure 6 indicates the onset of this scatter occurs at similar $T_{\rm eff}$ in the Hyades, and the magnitude of the scatter appears similar, though the presence of censored data (upper limits) complicates interpretation. What seems clear is that the star-to-star spread among the UMa group stars with Li detections is more similar to the modest spread evinced by non-tidally locked binaries in the older Hyades cluster than the large (up to a full dex) striking differences in similarly cool young (100-200 Myr) Pleiades and M34 cluster dwarfs (e.g., Figure 3 of Jones et al. 1997). Our new membership information thus verifies essentially similar conclusions of Soderblom et al. (1993b). Fig. 6

The Hyades Li data in Figure 6 were analyzed in the same fashion as our UMa stars, repeating the analysis of Balachandran (1995) with our particular choice of $T_{\rm eff}$ scale and model atmosphere grids, etc. Though UMa datapoints remain sparse, Figure 6 indicates that the Hyades Li abundances are lower than those in UMa for $T_{\rm eff} \leq 5400$ K. This difference increases modestly if NLTE corrections (Carlsson et al. 1994) are applied. The larger UMa Li content relative to cool Hyades would be further exaggerated if we were to utilize a mass coordinate, instead of $T_{\rm eff}$, since the masses are larger at a fixed temperature for higher metallicity like that characterizing the Hyades (e.g., [Fe/H]= +0.12 according to Cayrel, Cayrel de Strobel & Campbell 1985). Greater Li depletion in the cool Hyads is qualitatively consistent with their higher [Fe/H] and the well-known "metallicity" dependence of standard pre-main-sequence Li burning (e.g., Figure 3 of Chaboyer, Demarque & Pinsonneault 1995; table 2 and §3.4 of Piau & Turck-Chièze 2002); greater Li depletion would also be consistent with a very slightly older age for the Hyades and the effects main-sequence mixing (e.g., the age dependence of Li destruction seen in the rotational mixing models of fixed composition in Figure 12 of Chaboyer et al. 1995).

While the data are very limited, comparison of the stars hotter than the F-star Li gap in Figure 6 suggests little difference in the Hyades and UMa initial Li abundances. We have also noted the near-equality in the UMa and Hyades age, with an allowance that the Hyades might be (if anything) slightly older. It is then interesting to note that the ∼0.0 dex abundance difference between the cool Hyades dwarfs 5150 K and the cool UMa dwarfs at 4850 K in Figure 6 is considerably *smaller* than the near ∼1.0 dex difference predicted by the standard models in Figure 3 of Chaboyer et al. (1995) given these entities' metallicity difference. This suggests that there is a fourth parameter beyond mass, age, and [Fe/H] controlling relative Li depletion. Numerous candidates abound– helium abundance, detailed opacity mixtures (in particular the [α/Fe] ratio), accretion history, initial angular momentum and subsequent evolution thereof. Several of these factors are discussed and modeled in Piau & Turck-Chièze (2002), but (unfortunately) remain observationally ill-constrained.

Figure 7 compares our UMa Li abundances with those for Coma, which we analyzed in a homogeneous fashion with temperatures derived as for UMa using the photometry described before. The Coma Li equivalent widths were taken from cluster members in the studies of Ford et al. (2001), Soderblom et al. (1990), and Boesgaard (1987). The UMa-Coma comparison is of particular interest since these clusters have observationally indistinguishable age and [Fe/H]. Figure 7 indicates that the cool star Li abundances appear some ∼0.2 dex lower in Coma than the maximum abundances seen in UMa. A similar difference is inferred from the relative predicted-observed Li differences for each cluster, where these differences are measured using the curves from Figure 3 of Chaboyer et al. (1995) and the two Coma stars at 5200 K and the 3 UMa stars at 4850 K. In this case, however, the implications

of any inter-cluster Li difference for a fourth parameter are unconvincing: the UMa-Coma comparison in Figure 5 may reflect a constant offset; i.e., the abundance levels on the hotside of the Li gap and in the G-star Li peak (5800-6000 K) may also differ at the 0.2 dex level. Such a difference is suggestive of one in initial Li abundance rather than in mass-dependent Li depletion mechanisms. Fig. 7

3.4. Summary

Using existing and new spectroscopy, we revisit membership and abundances for stars in the UMa moving group. Comparison of the color-magnitude diagrams of UMa, Coma, and the Hyades using isochrones suggests that these stellar aggregates are essentially coeval, with the Hyades perhaps being only 100 Myr older. This finding provides a simple explanation for the modest scatter of UMa stars in the chromospheric emission versus color plane compared to younger clusters (e.g., the Pleiades), and the indistinguishable mean chromospheric emission levels of UMa and Hyades members.

Abundances from our new spectroscopy confirms non-membership for HD 81659. Our new spectroscopy of field star UMa group members reveals they clearly demonstrate abundance trends suggestive of or mimicing the effects of over-excitation/ionization that have been reported in young clusters and very active field stars: abundances derived from low excitation potential lines of a given species are lower than the abundances derived from higher excitation lines; at $T_{\rm eff}\sim$5000 K, Fe abundances derived from Fe II lines are a factor 4 higher than abundances derived from Fe I lines; O I abundances derived from the high excitation λ7774 triplet show an increase with decreasing $T_{\rm eff}$. This latter trend of rising O with declining $T_{\rm eff}$ is strikingly muted compared to that seen in younger and more metal-rich Pleiades stars.

Fe I-based Fe abundances for HD 28495 and 173950 are notably higher than the photometric metallicity estimates of Nordstrom et al. (2004). There are several UMa members for which Nordstrom et al. (2004) metallicities are markedly low compared to the canonical UMa abundance. Similar oddly low photometric estimates for cool stars are also seen in the Hyades, and the Nordstrom et al. (2004) photometric values yield a metallicity some 0.10-0.15 dex lower than the canonical spectroscopic metallicity in this cluster too.

For $T_{\rm eff}\geq$5200 K, UMa group member Li abundances show remarkably small dispersion that is compatible with the estimated errors. As in other young clusters, however, a significant star-to-star scatter in Li is seen at cooler $T_{\rm eff}$ values. Consistent redetermination of Hyades Li abundances indicates lower values at a given cool temperature (and

corresponding mass) than for UMa–a difference qualitatively consistent with expectations of standard PMS burning given the higher Hyades [Fe/H] value. However, the quantitative Hyades-UMa cool dwarf difference is considerably smaller than expected, suggesting a fourth parameter other than stellar mass, age, and [Fe/H] affecting the relative Li depletion in cool young-to-intermediate age open cluster dwarfs. Cool dwarfs in UMa and Coma, which have observationally indistinguishable age and [Fe/H], show only a modest $\leq$0.2 dex, if any, difference that could be due to an initial abundance difference.

Uniquely identifying this fourth parameter may be observationally challenging: the initial angular momentum distribution and details of angular momentum loss are both folded into the present day stellar rotation distributions (which may additionally be convolved with projection effects); observable signatures of accretion will quickly be lost by convective dilution in sufficiently low-mass stars; and stellar He abundances are notoriously difficult to determine (particularly in low mass stars). Differences in detailed opacity mixtures are the most amenable to observational discrimination, but consistent abundance analyses of numerous elements in large samples of open cluster stars do not yet exist. While this lack of important observational data seems easy to remedy, the abundance results presented here and the recent work indicating (presumably spurious) $T_{\rm eff}$- and/or age- and/or activity-dependent trends in cool dwarf abundances (Cayrel et al. 1985; King et al. 2000; Schuler et al. 2003,2004; Yong et al. 2004; Morel & Micela 2004) suggests the needed delineation of genuine cluster-to-cluster abundance differences is not necessarily straightforward. Indeed, an interesting future question is how any such effects influence the measured Li abundances in different clusters themselves.

The author gratefully acknowledges support for this work from NSF awards AST-0086576 and AST-0239518, and a generous grant from the Charles Curry Foundation to Clemson University. We also thank Dr. Aaron Steinhauer for kindly providing his LIFIND code, and Ms. Abigail Daane and Mr. Roggie Boone for their assistance at the McDonald 2.7-m and KPNO 4-m telescopes.

REFERENCES

Allende Prieto, C., Barklem, P. S., Lambert, D. L., & Cunha, K. 2004, A&A, 420, 183

Balachandran, S. 1990, ApJ, 354, 310

Balachandran, S. 1995, ApJ, 446, 203

Boesgaard, A. M., & Friel, E.D. 1990, ApJ, 351, 467

Boesgaard, A. M. 1989, ApJ, 336, 798

Boesgaard, A. M., Budge, K. G., & Burck, E. E. 1988, ApJ, 325, 749

Boesgaard, A. M., & Tripicco, M. J. 1987, ApJ, 313, 389

Boesgaard, A. M. 1987, ApJ, 321, 967

Carlsson, M., Rutten, R. J., Bruls, J. H. M. J., & Shchukina, N. G. 1994, A&A, 288, 860

Cayrel, R. 1988, in The Impact of Very High S/N Spectroscopy on Stellar Physics, ed. G. Cayrel de Strobel & M. Spite, (Dordrecht: Kluwer), p. 345

Cayrel, R., Cayrel de Strobel, G., & Campbell, B. 1985, A&A, 146, 249

Chaboyer, B., Demarque, P., & Pinsonneault, M. H. 1995, ApJ, 441, 876

Chen, Y. Q., Nissen, P. E., Benoni, T., & Zhao, G. 2001, A&A, 371, 943

de Bruijne, J. H. J., Hoogerwerf, R., & de Zeeuw, P. T. 2001, A&A, 367, 111

de Medeiros, J. R., & Mayor, M. 1999, A&AS, 139, 433

Deliyannis, C. P., Steinhauer, A., & Jeffries, R. D. 2002, ApJ, 577, L39

Deliyannis, C. P., King, J. R., Boesgaard, A. M., & Ryan, S. G. 1994, ApJ, 434, L71

Deliyannis, C. P., Boesgaard, A. M., Stephens, A., King, J. R., Vogt, S. S., & Keane, M. J. 1998, ApJ, 498, L147

Favata, F., Barbera, M., Micela, G., & Sciortino, S. 1995, A&A, 295, 147

Fekel, F. C. 1997, PASP, 109, 514

Ford, A., Jeffries, R. D., James, D. J., & Barnes, J. R. 2001, A&A, 369, 871

Gaidos, E. J., Henry, G. W., & Henry, S. M. 2000, AJ, 120, 1006

Henry, T. J., Soderblom, D. R., Donahue, R. A., & Baliunas, S. L. 1996, AJ, 111, 439

Fitzpatrick, M. J., & Sneden, C. 1987, BAAS, 19, 1129

Ford, A., Jeffries, R. D., James, D. J., & Barnes, J. R. 2001, A&A, 369, 871

Johnson, H. L., & Knuckles, C. F. 1955, ApJ, 122, 209

Jones, B. F., Fischer, D., Shetrone, M., & Soderblom, D. R. 1997, AJ, 114, 352

King, J. R., Krishnamurthi, A., & Pinsonneault, M. H. 2000, AJ, 119, 859

King, J. R., Villarreal, A. R., Soderblom, D. R., Gulliver, A. F., & Adelman, S. J. 2003, AJ, 125, 1980

King, J. R., Soderblom, D. R., Fischer, D., & Jones, B. F. 2000, ApJ, 533, 944

Lambert, D. L., Heath, J. E., & Edvardsson, B. 1991, MNRAS, 253, 610

Lèbre, A., de Laverny, P., de Medeiros, J. R., Charbonnel, C., & da Silva, L. 1999, A&A, 345, 936

Lejeune, Th., Cuisinier, F., & Buser, R. 1998, A&A, 130, 65

Morel, T., & Micela, G. 2004, A&A, 423, 677

Morel, T., Micela, G., Favata, F., & Katz, D. 2004, A&A, 426, 1007

Montes, D., López-Santiago, J., Fernández-Figueroa, M. J., & Gálvez, M. C. 2001, A&A, 379, 976

Nordstrom, B., Mayor, M., Andersen, J., Holmberg, J., Pont, F., Jorgensen, B. R., Olsen, E. H., Udry, S., & Mowlavi, N. 2004, A&A, 418, 989

Pallavicini, R., Randich, S., & Giampapa, M. S. 1992, A&A, 253, 185

Pallavicini, R., Cerruti-Sola, M., & D. K. Duncan 1987, A&A, 174, 116

Perryman, M. A. C., Brown, A. G. A., Lebreton, Y., Gomez, A., Turon, C., de Strobel, G., Cayrel, G., Mermilliod, J. C. et al. 1998, A&A, 331, 81

Piau, L., & Turck-Chieze, S. 2002, ApJ, 566, 419

Pinsonneault, M. H., Stauffer, J., Soderblom, D. R., King, J. R., & Hanson, R. B. 1998, ApJ, 504, 170

Randich, S., Gratton, R., Pallavicini, R., Pasquini, L., & Carretta, E. 1999, A&A, 348, 487

Rebolo, R., Beckman, J. E., Crivellari, L., Castelli, F., & Foing, B. 1986, A&A, 166, 195

Royer, F., Grenier, S., Baylac, M. O., Gomez, A. E., & Zorec, J. 2002, A&A, 393, 897

Russell, S. C. 1995, ApJ, 451, 747

Saar, S. H., & Osten, R. A. 1997, MNRAS, 284, 803

Schuler, S. C., King, J. R., Fischer, D. A., Soderblom, D. R., & Jones, B. F. 2003, AJ, 125, 2085

Schuler, S. C., King, J. R., Hobbs, L. M., & Pinsonneault, M. H. 2004, ApJ, 602, L117

Simon, T., & Landsman, W. 1991, ApJ, 380, 200

Soderblom, D.R., Jones, B.F., Balachandran, S., Stauffer, J.R., Duncan, D.K., Fedele, S.B., Hudon, J.D. 1993, AJ, 106, 1059

Soderblom, D. R., Pilachowski, C. A., Fedele, S. B., & Jones, B. F. 1993b, AJ, 105, 2299

Soderblom, D. R., & Mayor, M. 1993a, ApJ, 402, L5

Soderblom, D. R., King, J. R., & Henry, T. J. 1998, AJ, 116, 396

Soderblom, D. R., Pendleton, J., & Pallavicini, R. 1989, AJ, 97, 539

Soderblom, D. R., & Clements, S. D. 1987, AJ, 93, 920

Soderblom, D. R., & Mayor, M. 1993b, AJ, 105, 226

Soderblom, D. R. 1985, PASP, 97, 54

Soderblom, D. R., Duncan, D. K., & Johnson, D. R. H. 1991, ApJ, 375, 722

Soderblom, D. R., Oey, M. S., Johnson, D. R. H., & Stone, R. P. S. 1990, AJ, 99, 595

Steinhauer, A. 2003, Ph. D. dissertation, Indiana University

Strassmeier, K. G., Fekel, F. C., Bopp, B. W., Dempsey, R. C., & Henry, G. W. 1990, ApJS, 72, 191

Strassmeier, K. G., Washuettl, A., Granzer, T., Scheck, M., & Weber, M. 2000, A&AS, 142, 275

Swenson, F. J., Faulkner, J., Iglesias, C. A., Rogers, F. J., & Alexander, D. R. 1994, ApJ, 422, L79

Thevenin, F. 1990, A&AS, 82, 179

Tinney, C. G., McCarthy, C., Jones, H. R. A., Butler, R. P., Carter, B. D., Marcy, G. W., & Penny, A. J. 2002, MNRAS, 332, 759

Uesugi, A., & Fukuda, I. 1970, Contr. Astroph. Kwasan Obs. Univ., 189

Wolff, S., & Simon, T. 1997, PASP, 109, 759

Yi, S., Demarque, P., Kim, Y.-C., Lee, Y.-W., Ree, C. H., Lejeune, T., & Barnes, S. 2001, ApJS, 136, 417

Yong, D., Lambert, D. L., Allende Prieto, C., & Paulson, D. B. 2004, ApJ, 603, 697

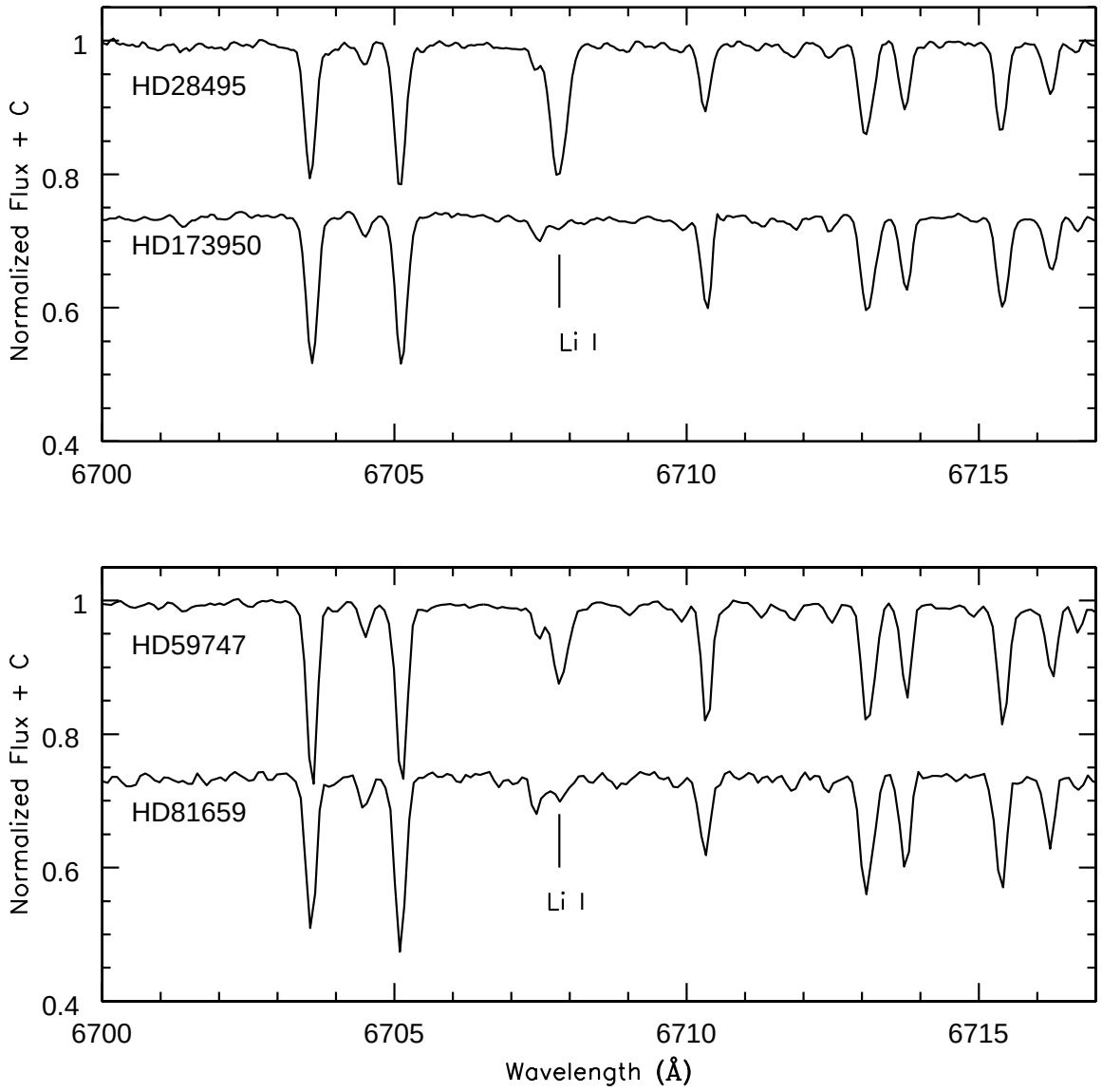

Fig. 1.— Sample spectra of our additional UMa candidates obtained at the McDonald Observatory 2.7m (top panel) and Kitt Peak National Observatory 4m (bottom panel).

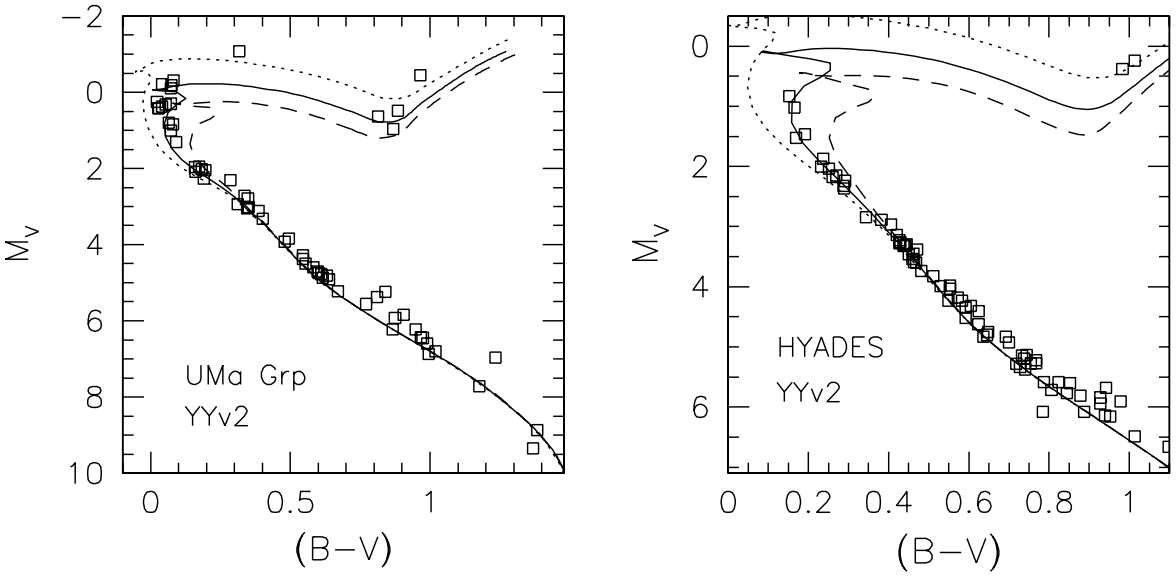

Fig. 2.— (Left) The Hipparcos-based UMa group color-magnitude diagram is shown with the 400, 600, and 800 Myr Yale-Yonsei [Fe/H]= −0.08 isochrones constructed with the Lejeune et al. (1998) color-temperature relation. (Right) The Hipparocs based Hyades color-magnitude diagram is shown with the 500, 700, and 900 Myr Yale-Yonsei [Fe/H]= +0.13 isochrones constructed with the same color-temperature relation.

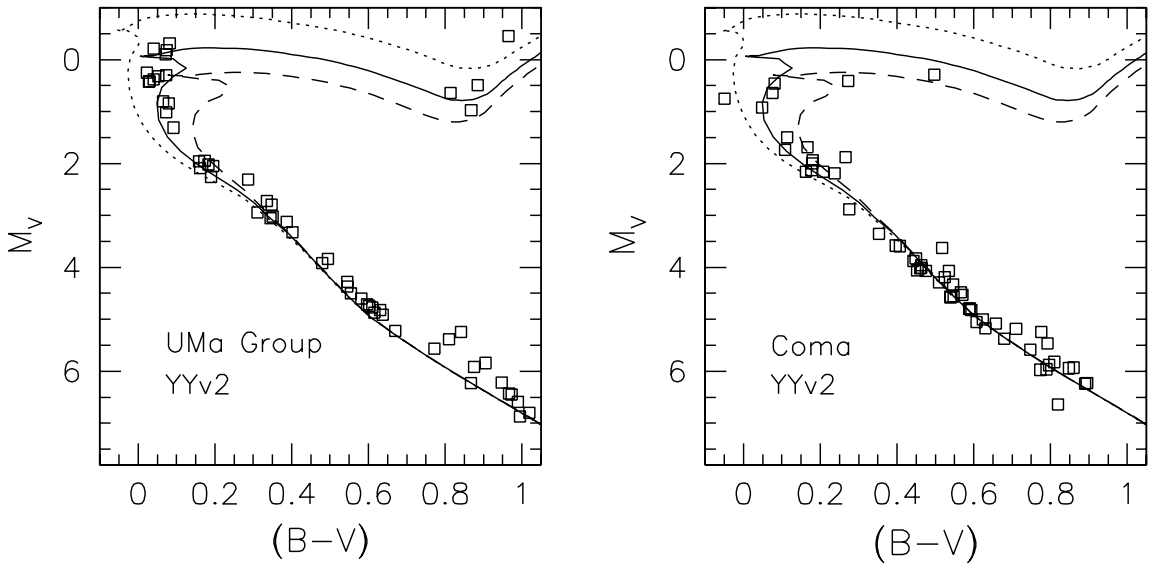

Fig. 3.— (Left) The UMa color magnitude diagram from Figure 1 is shown again. (Right) The Coma color-magnitude diagram, assuming $(m - M) = 4.54$ and $E(B - V) = 0.00$, is plotted with the same 400, 600, and 800 Myr [Fe/H]= −0.08 isochrones as for UMa.

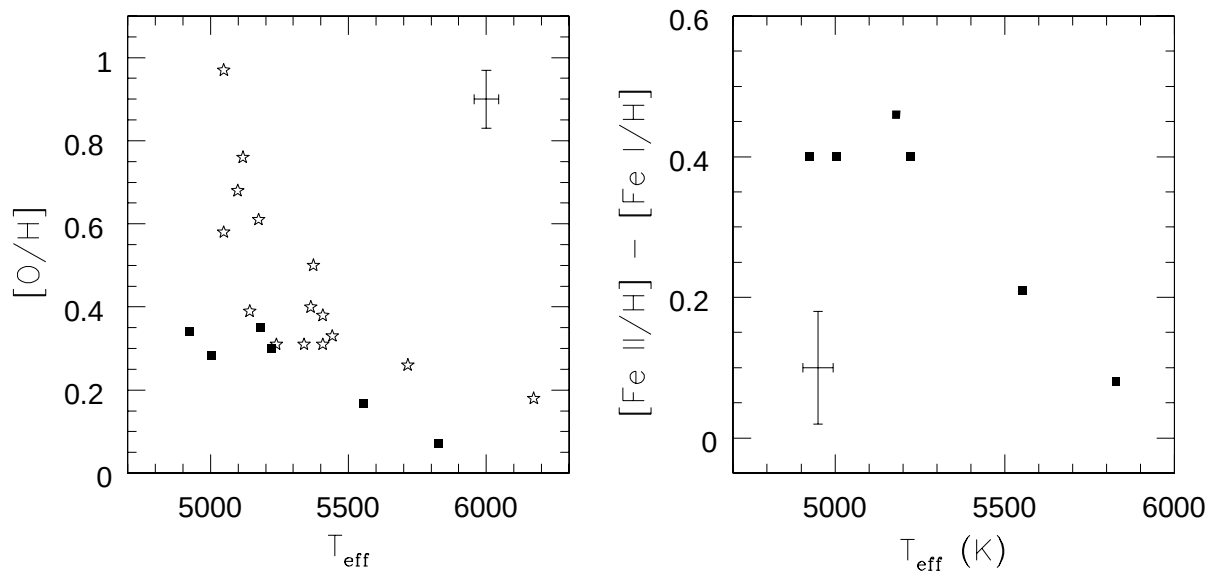

Fig. 4.— Left– The λ7774 O I-based [O/H] values from our own spectroscopy are plotted versus $T_{\rm eff}$ for UMa group objects (filled squares) and Pleiades dwarfs from Schuler et al. (2004; open stars); a typical error bar is shown in the upper right. Right– The difference between [Fe/H] determined from Fe II and Fe I lines based on our own spectroscopy of UMa group objects. A typical error bar is shown in the bottom left.

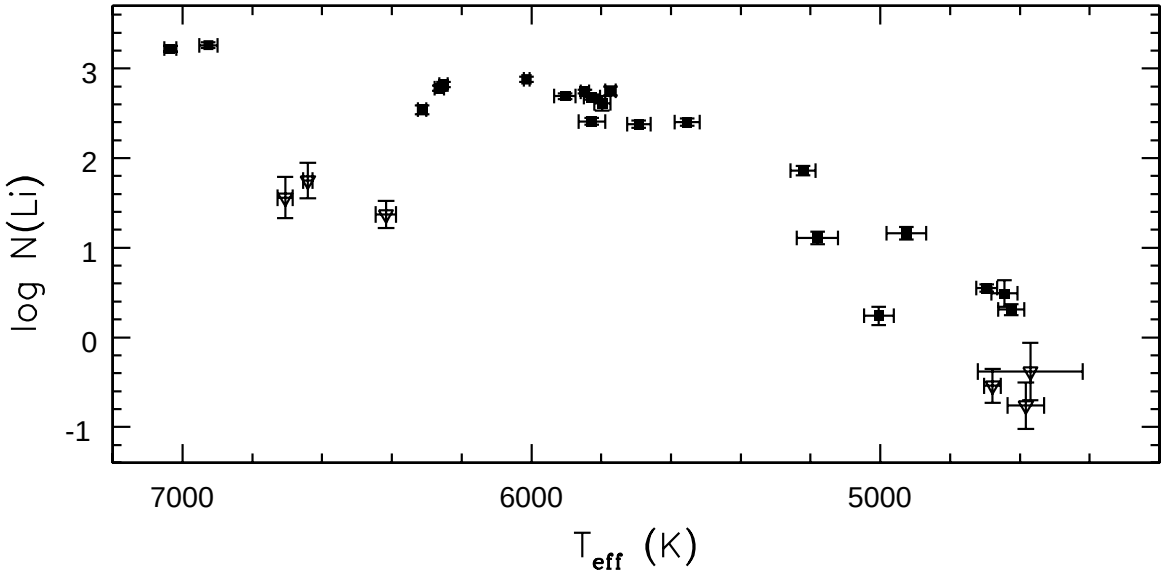

Fig. 5.— LTE Li abundance is plotted versus $T_{\rm eff}$ for our UMa objects. Upper limits are shown as inverted open triangles.

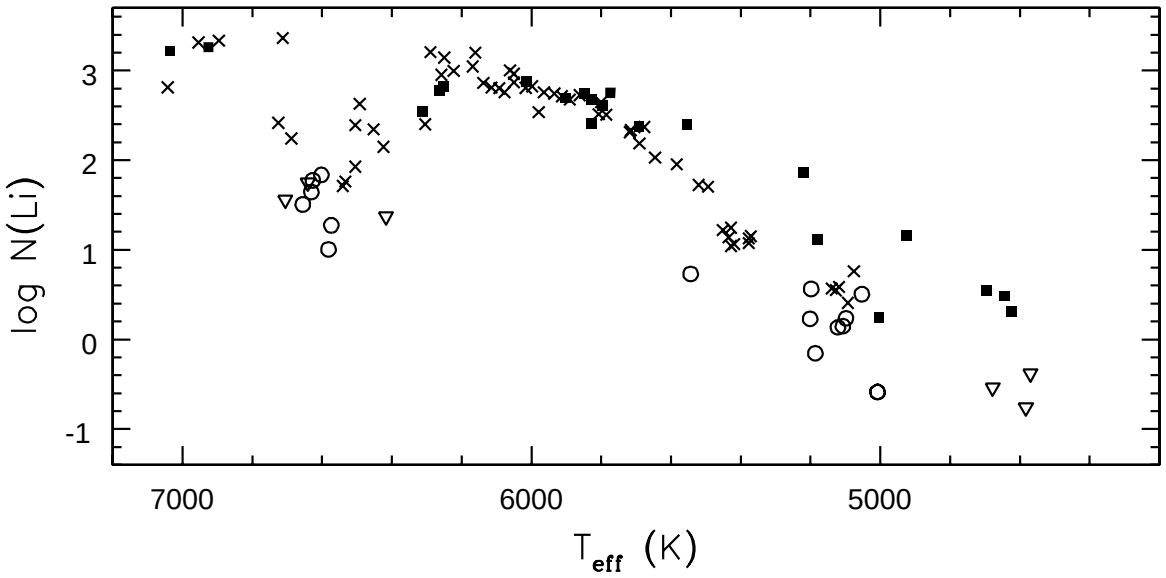

Fig. 6.— LTE Li abundances for the Hyades (crosses and open circles; the latter designating upper limits) and our UMa objects (symbols the same as in Figure 3) are shown versus $T_{\rm eff}$.

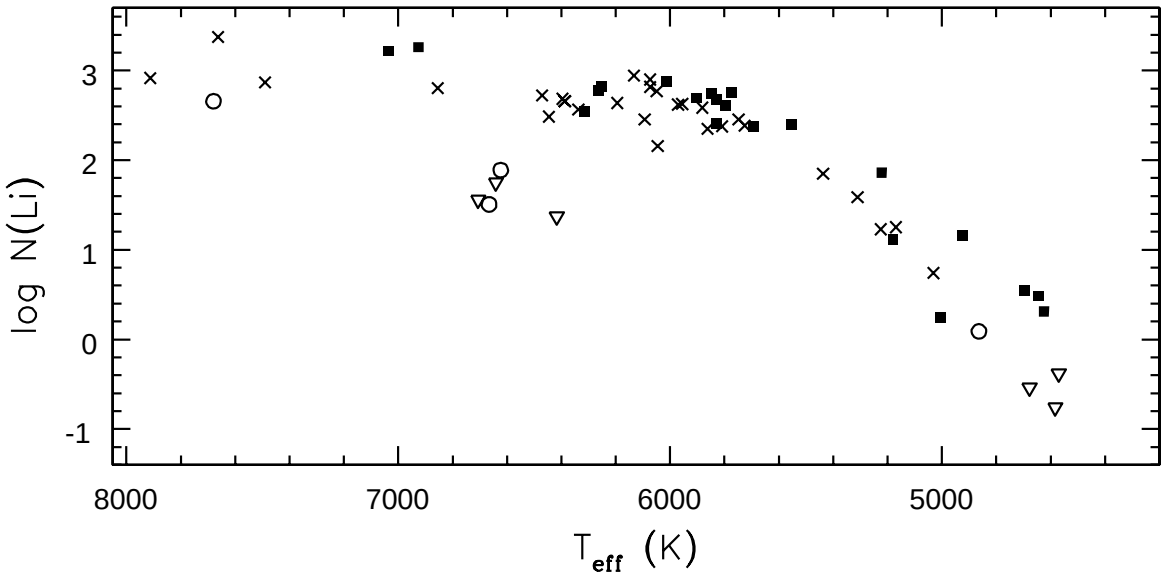

Fig. 7.— LTE Li abundances for Coma Berenices (crosses and open circles denote detections and upper limits) and our UMa objects (with symbols as in Figure 3) are shown versus $T_{\rm eff}$.

Table 1. UMa Group Fe I Line Data

λ Å	χ eV	log gf	HD28495 mÅ	HD59747 mÅ	HD63433 mÅ	HD75935 mÅ	HD81659 mÅ	HD167389 mÅ	HD17395 mÅ
6703.58	2.76	-3.13	49.9	65.3	···	54.2	53.7	35.5	56.
6713.75	4.79	-1.52	24.3	31.8	25.6	28.7	33.1	19.6	27.
6725.36	4.10	-2.30	22.4	30.4	23.9	26.1	27.0	16.9	24.
6726.67	4.61	-1.12	55.0	69.4	57.4	62.3	58.5	48.1	57.
6739.52	1.56	-4.98	21.6	33.7	14.7	26.4	23.8	10.6	26.
6745.98	4.07	-2.74	8.4	13.5	6.7	10.8	12.0	6.2	9.
6746.98	2.61	-4.35	6.6	11.6	6.7	7.5	9.0	···	9.

Table 2. UMa Group Parameters and Fe Abundance Data

	HD28495	HD59747	HD63433	HD75935	HD81659	HD167389	HD173950	Sun
Parameters								
$T_{\rm eff}$	5222	4925	5553	5180	5467	5827	5004	5770
log g	4.62	4.65	4.57	4.63	4.58	4.52	4.65	4.44
ξ	1.14	1.04	1.25	1.12	1.22	1.36	1.07	1.38
[m/H]	-0.2	-0.10	-0.10	-0.10	+0.10	-0.10	-0.20	+0.00
Abundances								
6703.58	-0.18	+0.01	···	-0.10	+0.04	-0.03	-0.16	7.59
6713.75	-0.16	+0.02	-0.02	-0.05	+0.11	-0.05	-0.09	7.59
6725.36	-0.17	+0.00	+0.01	-0.07	+0.04	-0.04	-0.15	7.62
6726.67	-0.15	+0.06	+0.02	-0.02	+0.02	-0.01	-0.14	7.56
6739.52	-0.21	+0.08	-0.13	-0.11	+0.05	-0.03	-0.21	7.57
6745.98	-0.20	+0.02	-0.16	-0.07	+0.07	-0.05	-0.18	7.55
6746.98	-0.19	-0.01	+0.04	-0.13	+0.12	···	-0.12	7.47
Results								
[Fe/H]	-0.18	+0.03	-0.04	-0.08	+0.06	-0.04	-0.15	7.564
std dev	0.020	0.033	0.084	0.038	0.037	0.015	0.039	0.048

Table 3. Supplemental Line Data

Species	λ Å	χ eV	log gf	Sun EW(mÅ)	HD75935 EW(mÅ)	HD59747 EW(mÅ)	HD173950 EW(mÅ)
Ca I	6417.69[a]	4.44	-0.75	15.0	18.0	22.6	19.3
	6449.82	2.52	-0.62	109.0	134.0	156.9	145.7
	6455.61	2.52	-1.50	58.9	75.0	93.4	82.5
	6464.68	2.52	-2.53	15.2	22.6	34.9	27.4
	6499.65	2.52	-1.00	89.7	111.0	126.5	121.7
Cr I	6330.10	0.94	-2.99	30.8	51.2	71.8	59.3
	6661.08	4.19	-0.24	13.0	···	28.1	23.6
	6729.75	4.39	-0.66	3.6	5.4	6.7	5.8
Fe I	6498.95	0.96	-4.70	50.0	69.2	83.5	75.1
	6608.04	2.28	-4.02	19.7	31.3	40.1	33.9
	6609.12	2.56	-2.67	71.1	87.7	99.9	90.8
Fe II	6416.93	3.89	-2.86	45.2	39.5	34.6	32.0
Ni I	6327.60	1.68	-3.23	40.6	54.0	60.5	49.2
	6378.26	4.15	-1.00	34.3	37.6	38.3	34.6
	6414.59	4.15	-1.29	20.0	23.9	21.2	20.6
	6482.81	1.93	-2.97	45.1	52.8	57.2	···
	6532.88	1.93	-3.47	18.4	27.6	31.3	23.5
	6598.61	4.23	-1.02	27.5	31.8	28.5	27.5
	6635.14	4.42	-0.87	27.3	29.7	28.0	24.8
	6767.78	1.83	-1.89	83.5	94.3	105.4	95.6

[a]Appea
is account
of the lin

Table 4. Supplemental Abundance Results

Species	λ Å	Sun log N	HD75935 [X/H]	HD59747 [X/H]	HD173950 [X/H]
Ca I	6417.69	6.63	-0.10	-0.07	-0.13
	6449.82	6.31	-0.24	-0.31	-0.33
	6455.61	6.44	-0.19	-0.16	-0.24
	6464.68	6.59	-0.20	-0.15	-0.23
	6499.65	6.41	-0.19	-0.28	-0.27
mean [Ca/H]			-0.18	-0.19	-0.24
std dev			0.051	0.099	0.073
Cr I	6330.10	5.78	-0.27	-0.20	-0.23
	6661.08	5.71	···	-0.01	-0.08
	6729.75	5.71	-0.08	-0.08	-0.12
mean [Cr/H]			-0.18	-0.10	-0.14
std dev			···	0.096	0.077
Fe I	6498.95	7.54	-0.20	-0.10	-0.23
	6608.04	7.57	-0.15	-0.07	-0.19
	6609.12	7.49	-0.10	-0.03	-0.16
mean [Fe/H][a]			-0.10	-0.00	-0.16
std dev			0.052	0.055	0.042
Fe II	6416.93	7.75	+0.40	+0.59	+0.37
Ni I	6327.60	6.37	-0.05	+0.01	-0.22
	6378.26	6.44	-0.04	+0.01	-0.10
	6414.59	6.40	0.00	-0.03	-0.09
	6482.81	6.43	-0.13	-0.10	···
	6532.88	6.36	-0.02	-0.03	-0.23
	6598.61	6.38	0.00	-0.02	-0.09
	6635.14	6.41	-0.03	-0.02	-0.13
	6767.78	5.92	-0.11	-0.03	-0.18
mean [Ni/H]			-0.05	-0.03	-0.15
std dev			0.048	0.034	0.061

[a]Includes the results for Fe features in Table2.

Table 5. UMa LTE O I Abundances

Quantity	λ7772	λ7774	λ7775
log gf	+0.333	+0.186	-0.035
Solar EW(mÅ)	73.7	63.8	50.1
log $N(\mathrm{O})_\odot$	8.94	8.93	8.91
HD28495 EW	52.2	42.7	32.4
[O/H]	+0.31	+0.29	+0.30
HD59747 EW	30.9	28.0	18.5
[O/H]	+0.32	+0.39	+0.32
HD63433 EW	65.8	58.1	45.5
[O/H]	+0.14	+0.17	+0.19
HD75935 EW	49.0	42.3	33.1
[O/H]	+0.33	+0.36	+0.39
HD167389 EW	82.0	71.5	55.6
[O/H]	+0.07	+0.07	+0.07
HD173950 EW	33.8	28.0	23.3
[O/H]	+0.25	+0.25	+0.35

Table 6. UMa Fe II Abundances

Quantity	λ6149.25	λ6247.56	λ6416.93	λ6456.39
log gf	-2.72	-2.31	-2.86	-2.08
Solar EW(mÅ)	38.2	56.6	45.2	67.7
log $N(\mathrm{Fe})_\odot$	7.47	7.44	7.75	7.43
HD28495 EW	28.7	46.3	34.7	59.1
[Fe/H]	+0.18	+0.23	+0.19	+0.28
HD59747 EW	22.2	32.7	34.6	43.1
[Fe/H]	+0.35	+0.30	+0.59	+0.35
HD63433 EW	40.7	55.1	41.6	67.6
[Fe/H]	+0.23	+0.16	+0.10	+0.19
HD75935 EW	29.8	49.1	39.5	57.8
[Fe/H]	+0.29	+0.38	+0.40	+0.35
HD167389 EW	40.2	62.0	43.8	72.2
[Fe/H]	+0.03	+0.10	-0.04	+0.08
HD173950 EW	20.6	34.2	32.0	45.3
[Fe/H]	+0.16	+0.19	+0.37	+0.25

Table 7. UMa Group Li Data

Star HD	[Fe/H] Phot	[Fe/H] Spect	$(B-V)$	$T_{\rm eff}$ K	EW(Li) mÅ	Li Ref	log N(Li) LTE	log $R'_{\rm HK}$	R
11131	-0.27	-0.10	0.638	5692±34	67.5	1,2		−4.50	3,
					78.0[a]	7,8,9	2.38±0.04		
13959A			0.995	4570±150	≤6[b]	1	≤ − 0.38±0.32	−4.35	
26923	-0.08	+0.08	0.582	5904±31	84.3	1,2,10,11	2.69±0.03	−4.50	2,
38393	+0.01	-0.07	0.495	6252±12	66.5	13,14		−4.77	
					58.5[a]	1,16	2.82±0.03		
38392			0.954	4678±24	≤3	1,16	≤ − 0.54±0.19	−4.48	5,1
39587	-0.06	-0.04	0.597	5847±12	100.3	14,19		−4.41	3
					102.8[a]	1,8	2.74±0.02		
72905	-0.20	-0.05	0.616	5774±15	108.5	2		−4.37	2,
					116.9[a]	1,8,22,23	2.75±0.05		
109011			0.948	4695±30	23.4	1,2	0.55±0.04	−4.37	2,
109647			0.967	4644±37	25.0	1	0.49±0.15	−4.45[c]	3,
109799	-0.24	-0.08	0.336	6926±26	56.0[a]	8	3.26±0.03	−4.36[d]	2
110463			0.974	4625±37	18.0	1	0.31±0.06	−4.43[c]	3,6
111456	-0.18		0.480	6313±12	36[a]	1	2.54±0.05	−4.38[d]	6,
115043	-0.19	-0.03	0.610	5797±23	77[e]	1		−4.45	3
					101[a]	22	2.61±0.08		
125451A	-0.02	-0.02	0.402	6641±13	≤3.9[a]	8	≤1.750±0.20	−4.37[d]	2
129798A	+0.00		0.387	6706±22	≤2.4[a]	29	≤1.56±0.23	···	
141003B			0.99	4583±52	≤2	1	≤ − 0.76±0.26	−4.38[c]	1
147584	-0.08	-0.19	0.554	6014±8	101	31		−4.56	
					93	33	2.88±0.03		
165185	-0.21	-0.06	0.602	5827±23	92.7	2		−4.45	2
					93.0	1	2.68±0.03		
180777			0.311	7035±17	45.4[a]	8	3.22±0.03	-4.34[d]	2
184960	-0.32	-0.14	0.492	6264±13	57.0	1,34		−5.07[c]	1
					61.6[a]	8	2.78±0.03		
211575	+0.09		0.455	6417±29	≤2.7	35	≤1.37±0.15	−4.71	3

New Data

Table 7—Continued

Star HD	[Fe/H] Phot	[Fe/H] Spect	$(B-V)$	$T_{\rm eff}$ K	EW(Li) mÅ	Li Ref	log N(Li) LTE	log $R'_{\rm HK}$	Ref	$v \sin i$ km/s	
28495	-0.41	-0.18	0.772	5222±36	71.5	38	1.86±0.05	−4.39	3		
59747	-0.14	-0.00	0.867	4925±57	41.0	39	1.16±0.07	−4.44	3		
63433	-0.10	-0.04	0.676	5553±36	99.6	39	2.40±0.04	−4.42	3		
75935		-0.10	0.785	5180±59	21.9	39	1.11±0.07	−4.44	3		
81659	+0.13	+0.06	0.700	5467±49	17.2	39	1.32±0.09	−4.57	3		
167389	-0.11	-0.04	0.602	5827±38	58.8	38	2.41±0.04	−4.74	3		
173950	-0.43	-0.16	0.841	5004±43	5.8	38	0.24±0.10	−4.46	3		

References. — (1) Soderblom et al. (1993); (2) Gaidos, Henry & Henry (2000); (3) King et al. (20 (4) Tinney et al. (2002); (5) Henry et al. (1996); (6) Soderblom & Mayor (1993a); (7) Pallavicini, Ran & Giampapa (1992); (8) Boesgaard, Budge & Burck (1988); (9) Boesgaard & Tripicco (1987); (10) Favat al. (1995); (11) Randich et al. (1999); (12) Lèbre et al. (1999); (13) Soderblom, King & Henry (1998); (14) C et al. (2001); (15) Soderblom, Pendleton & Pallavicini (1989) ; (16) Pallavicini, Cerruti-Sola & Duncan (19 (17) Soderblom & Mayor (1993b); (18) Soderblom & Clements (1987); (19) Lambert, Heath & Edvard (1991); (20) Strassmeier et al. (1990); (21) Fekel (1997); (22) Montes et al. (2001); (23) Wichmann, Schmi Hubrig (2003); (24) Simon & Landsman (1991); (25) Uesugi & Fukuda (1970); (26) Strassmeier et al. (20 (28) de Medeiros & Mayor (1999); (29) Russell (1995) (30) Royer et al. (2002); (31) Rebolo et al. (1986); Saar & Osten (1997); (33) Soderblom (1985); (34) Balachandran (1990); (35) Deliyannis et al. (1998); Soderblom, Duncan, & Johnson (1991); (37) Wolff & Simon (1997); (38) McDonald 2.7-m; (39) KPNO 4-

[a]Equivalent width measurement contains a contribution from the nearby 6707.4Å Fe I+CN blending feat

[b]Review of the resolved photometry in Fabricius & Makarov (2000) suggests the close components of 13959AB have near equal brightness at 6700 Å. The original equivalent width upper limit has thus been dou to account for continuum dilution.

[c]The log R'$_{hk}$ index from (18) has been transformed to log R'$_{HK}$ using their relations.

[d]The log R'$_{1335}$ index from (24) has been transformed to log R'$_{hk}$ and then to log R'$_{HK}$ using the relat in (18).

[e]The 77 mÅ equivalent width from (1) differs substantially from the Fe-corrected equivalent width of 96 from (22).